Cargo Transport Shapes the Spatial Organization of a Microbial Community

Authors: Abhishek Shrivastava[1,2,3], Visha K. Patel[1], Yisha Tang[1], Susan Connolly Yost[2], Floyd E. Dewhirst[2] and Howard C. Berg[1,3]

Affiliations:

[1] Department of Molecular and Cellular Biology, Harvard University, Cambridge, MA, USA.

[2] The Forsyth Institute, Cambridge, MA, USA.

[3] The Rowland Institute at Harvard, Cambridge, MA, USA.

Email: hberg@mcb.harvard.edu, ashrivastava@fas.harvard.edu

Abstract: The human microbiome is an assemblage of diverse bacteria that interact with one another to design a community. Bacteria that form a community are arranged in a three-dimensional matrix with many degrees of freedom. Snapshots of microbial communities display well-defined structures but how a non-ordered community reaches an ordered state is not clear. Bacterial gliding is defined as the motion of cells in a screw-like fashion over an external surface. Genomic analysis suggests that gliding bacteria are abundant in human microbial communities. Gliding bacteria require a functional bacterial Type IX Secretion System, and a motility machinery that propels the mobile cell-surface adhesin SprB. Here we report that cells of abundant non-motile bacteria found in human oral microbial communities attach to single gliding bacterial cells via SprB. The attached non-motile bacteria are propelled as 'cargo' along the length of a gliding cell. Multi-color fluorescent spectral imaging of live bacterial cells within a polymicrobial community shows long-range transport of non-motile cargo bacteria by a moving swarm. Tracking of fluorescently labeled single cells and of fluid flow patterns via gas bubbles suggests hierarchy within a swarm. We find that the synchronized public transport of cargo bacteria provides a specific spatial structure to a polymicrobial community, and that some non-motile bacteria use public transport more efficiently than other members of their community.

Introduction. Bacteria that attach to and colonize a surface form some of the most stable species of the human microbiome. Rapid availability of nutrition, protection from antibiotics, and long-term colonization are advantages of attaining a specific spatial niche within a microbial community. The mechanisms that drive interactions and guide the architecture of microbial communities are unclear. Active motion via the help of a molecular motor and guidance by a chemotaxis pathway enables a bacterium to sense its environment and find a spatial niche[1,2]. While the chemotaxis ability of a bacterium improves surface colonization[3,4], motile bacteria do not dominate a microbiome. Non-motile bacteria can reach a spatial niche via diffusion or a flow of fluid. A non-motile spherical bacterial cell with a radius 1 μm has a diffusion coefficient (D) = 2 x 10^{-9} cm^2/s. The time (t) taken by the cell to diffuse a certain distance (L) can be computed by the equation t = L^2/D. This bacterial cell would take 5 hours to diffuse to a distance of 60 μm and about 166 hours to diffuse to a distance of 120 μm. Thus, diffusion is not an efficient means of transport for a cell that has a size of few microns. Fluid flows that are encountered by microbial communities can be erratic. Neither diffusion nor fluid flows appear to be the major reason for arrangement of a microbial community into reproducible spatial structures. Another possible way by which non-motile bacteria get transported is by hitchhiking a ride on motile microorganisms[5,6]. Only few examples of hitchhiking are known[5,6] and the overall significance of hitchhiking is unclear. Whether hitchhiking is found in polymicrobial communities is not known. We describe a widespread mechanism of hitchhiking where motile but non-flagellated bacteria that are a part of the human microbiome carry non-motile bacteria as cargo. This mechanism of public transport is used by a diverse set of bacterial species that are abundant in the human microbiome.

Collective motion and swarm behavior are observed in biological objects of all sizes, such as bacteria, insects, birds, and fish[7,8]. The transition of an isolated cell to a swarm can be broadly explained by models based on phase transitions[9]. Variations in adhesion forces, the mode of motility, and a bias in the direction of motion govern the swarm behavior of a particular species. Swarms of flagellated bacteria comprise dense groups of cells that move in a thin layer of liquid close to a surface. However, in order to swarm, these bacteria do not need to be in contact with that surface[9,10]. Motile but non-flagellated bacteria that have either mobile cell-surface adhesins or the type 4 pili swarm with the cell-body in contact with an external surface. Bacteria that use motor-driven mobile cell-surface adhesins for motility are classified as gliding bacteria. Bacterial gliding requires a continuous expenditure of energy, and it only occurs when the bacteria are in contact with an external surface, with cells moving actively in a screw-like fashion[11-13].

Bacteria of the phyla Bacteroidetes are abundant in human gut and oral microbiomes and many members of this phyla have the ability to navigate surfaces via gliding motility. The Bacteroidetes represent about half of the bacterial population of the human gut microbiome[14,15] and changes in their concentration correlates with diseases such as obesity, diabetes and colitis[16-18]. The Type IX Protein Secretion System (T9SS) is found in many Bacteroidetes and is required for the secretion of proteins such as cell-surface adhesins, chitinase, cellulase, and proteases. T9SS is found in both motile and non-motile Bacteroidetes. The core T9SS proteins are SprA, SprE, SprT, and GldK-N. Bacteria with a cell-surface adhesin SprB, motility proteins GldA-B, GldD, GldF-J, and a functional T9SS are able to move over external surfaces[19].

The human oral microbiome is a catalog of microorganisms from lips, teeth, gingiva,

tongue, cheek, palate, and contiguous extensions of the oral cavity[20]. Bacteroidetes of the genus *Porphyromonas*, *Prevotella*, and *Capnocytophaga* are found in abundance in the human oral microbiome, and they contain the genes to encode the T9SS. Several reports show the abundance of *Capnocytophaga sp.* in different sites of the human oral microbiome[21-24]. Some *Capnocytophaga sp.* isolated from the human oral microbiome are known to exhibit gliding motility[25], and cells lacking the T9SS are deficient in gliding[26]. All *Capnocytophaga sp.* isolated from the human oral microbiome possess the genes to encode the T9SS and its associated gliding machinery. This suggests that the mechanism of gliding found in the phyla Bacteroidetes is prevalent in the genus *Capnocytophaga*. However, no experimental data exist about the mechanism for the motion of single cells of the genus *Capnocytophaga*. Motile cells in a community often move as a swarm but nothing is known about the swarm behavior of any gliding Bacteroidetes.

Recently, via fluorescent labeling of fixed samples of human oral biofilms, Welch *et al.* showed the presence of a structured and multigenus consortia within human oral microbial communities[22]. How a non-ordered community reaches an ordered state and arranges itself into spatial structures is not clear. Sequence and imaging data showed that bacteria of the *Capnocytophaga* genus are found in abundance in both human supragingival and subgingival biofilms[22]. Why the members of a genus that represents gliding bacteria are stable and abundant in the oral microbiome of a healthy human is not known. Via spectral imaging of live cells, we analyze the evolution of a polymicrobial community that contains eight abundant bacterial species of a human subgingival biofilm. We show that swarming *Capnocytophaga* shape a polymicrobial community by acting as vehicles of public transport and that patterns within a microbial community arise as a

result of this active motion. Over longer time scales, a combination of active motion and cell growth can shape the spatial features of a microbial community.

Results & Discussion.

Cooperation amongst abundant bacteria of the human oral microbiome is promoted by cargo transport. Genes that encode the bacterial T9SS and a cell surface adhesin SprB are present in *Capnocytophaga gingivalis*, which is abundant in human oral biofilms. *C. gingivalis* belongs to the phylum Bacteroidetes and is related to the environmental model gliding bacterium *Flavobacterium johnsoniae*. Addition of an antibody raised against the SprB of *F. johnsoniae* to a culture of *C. gingivalis* caused cell aggregation (Fig. S1). To test the hypothesis that the adhesin SprB of a gliding bacterium could bind to the cell-surface of non-motile bacteria, seven abundant and non-motile bacterial species found in human subgingival biofilms were co-cultured with gliding *C. gingivalis*. The non-motile bacteria were *Porphyromonas endodontalis*, *Prevotella oris*, *Parvimonas micra*, *Actinomyces sp.* oral taxon-*169*, *Fusobacterium nucleatum*, *Streptococcus sanguinis*, and *Veilonella parvula*. Cell of the non-motile bacterial species attached to the cell-surface of *C. gingivalis* and were transported as cargo along the length of a *C. gingivalis* cell from one pole to another (Fig. 1A and Movie S1-S7). The adhesin SprB of *F. johnsoniae* moves in a spiral fashion on the cell-surface[11]. The trajectory of the path travelled by a non-motile bacterium on the surface of a *C. gingivalis* is similar to the trajectory of the adhesin SprB (Fig. 1B). During their natural lifestyle, bacteria of the human microbiome encounter surfaces that are composed of tissue of varying stiffness. Such surfaces are often layered with mucus and are colonized by a

6

polymicrobial community. The adhesin SprB enables binding of a bacterial cell to polysaccharides. Bacterial cells surfaces are abundant in polysaccharides and the SprB adhesin of *C. gingivalis* might bind to the cell-surface polysaccharides of non-motile bacteria.

T9SS and its associated rotary motor are functional in gliding bacteria of the human microbiome. Some *C. gingivalis* cells tethered to a glass surface and rotated about fixed axes at speeds about 1.5 Hz. (Fig. 2A-B and Movie S8). Rotation of a tethered *F. johnsoniae* cell around a fixed axis is attributed to the presence of a rotary motor that is coupled to T9SS[29]. Cells that did not tether to glass by one adhesin glide long distances[29]. Some C. gingivalis cells that were able to glide over a glass surface moved at speeds of about 1 µm/s (Fig. 2C and Movie S9). *sprA*, *sprE*, *sprT*, and *gldK-N* genes encode the proteins that form the core T9SS. *gldA*-B , *gldD*, and *gldF-J* encode proteins that associate with the T9SS to enable gliding motility. The environmental gliding bacterium *F. johnsoniae* has all 15 genes. T9SS is found in many Bacteroidetes and one study identified T9SS in 62% of the sequenced species of the phyla Bacteroidetes[30]. *Capnocytophaga* species found in the human oral microbiome have all T9SS and gliding motility genes. Of the seven abundant non-motile bacteria used in this study, *P. endodontalis* and *P. oris* have T9SS genes but they lack the gliding motility genes (Fig. 2D). These observations combined with the presence of all T9SS-gliding motility genes and mobile cell-surface adhesins demonstrate that the machinery that enables gliding motility of members of the Bacteroidetes phyla is functional in *C. gingivalis*.

Gliding bacteria from the human microbiome display synchronized swarm behavior. *C. gingivalis* cells displayed swarm behavior over an agar surface. Such

swarms moved in a synchronized manner and circular motion of cells was observed near the edge of the swarm. Their motion was tracked with micron sized gas bubbles with surfactant walls. Such bubbles floated on the top layer of the swarm. (Fig. 3A-B and Movie S10). The gas bubbles near the leading edge of a swarm moved in circular trajectories predominantly in the counter-clockwise direction (Fig. 3C). The speed of bubbles, which is also the speed of the top layer of the swarm, was around 18 µm/min. (Fig. 3D).

Speeds of layers of a swarm are additive. The swarms of *C. gingivalis* seemed to form layers which were superimposed on top of one other. If layers move in similar directions and cells in the bottom layer move with a speed *v*, then cells in the upper layer would move with a speed *2v*. To test this hypothesis, a small percentage of fluorescently labeled *C. gingivalis* cells were mixed with unlabeled *C. gingivalis* cells. Fluorescently labeled cells were tracked in a swarm containing both labeled and unlabeled cells (Fig. 4 inset and Movie S11). The speed distribution of cells was bimodal with peaks around both 9 and 18 µm/min (Fig. 4A). Small groups of cells or 'slugs' that appeared near the edge of a swarm were tracked and their speed was around 9 µm/min (Fig. 4B-C and Movie S12). This suggests that the speed of a swarming cell and its synchronization correlates with its location in a three-dimensional spatial domain.

Counter-clockwise motion of a swarm can be explained from the right-handed motion of single cells. Single gliding cells move in a manner similar to a right handed screw. If the front end of a flexible gliding cell moving as a right handed screw sticks to an external surface, the cell body bends resulting in the front end of the cell pointing towards the left (Fig 4D and S2). Models that explain group behavior suggest that in a group, the direction of motion of an individual cell depends on the direction of motion of

8

its neighbors and perturbations in the noise of the system result in varying patterns of a swarm[8]. Cells that are in the vicinity of a bent cell move along the direction of the bend, and this direction of motion gets propagated in a swarm, thus resulting in its counter-clockwise motion (Fig. 4D).

Long-range cargo transport shapes a microbial community. The spatial localization of bacteria was studied in a polymicrobial community comprising *C. gingivalis* and seven non-motile bacterial species. The non-motile bacteria used in the study were: *Porphyromonas endodontalis*, *Prevotella oris*, *Parvimonas micra*, *Actinomyces sp.* oral taxon-*169*, *Fusobacterium nucleatum*, *Streptococcus sanguinis*, and *Veilonella parvula*. All eight bacteria of this polymicrobial community are found in abundance in a human subgingival biofilm. Single cells of the non-motile bacteria establish a cargo-transporter relationship with single *C. gingivalis* cells (Fig.1A). To explore if *C. gingivalis* swarms had the capability to transport the non-motile bacteria over long distances, the cell surfaces of the non-motile bacteria were labeled using seven different Succinimidyl Ester Alexa Flour fluorescent dyes. Physiological features, such as the motility of labeled *C. gingivalis* remained unaltered, thus providing a powerful tool for live-cell imaging. A polymicrobial community containing seven fluorescently labeled non-motile bacteria and gliding *C. gingivalis* was imaged, and spectral imaging was used to separate the fluorescent signals. Long-range transport of non-motile bacteria by swarming *C. gingivalis* was observed in a polymicrobial community (Fig. 5A and Movie S13). Within 20 minutes, the polymicrobial community evolved in such a way that many non-motile bacteria were arranged as islands surrounded by swarms *C. gingivalis* and some non-motile bacteria (Fig. 5A). The non-motile bacteria were actively transported via the swarms as cargo (Fig. 5B). Polymicrobial

9

aggregates of non-motile bacteria were transported by *C. gingivalis*. Such aggregates changed their structures while moving with a swarm (Fig. 5C). Tracking of individual bacterial species revealed that some non-motile bacteria moved distances of upto 30 μm in a swarm. Some non-motile bacteria, such as *Fusobacterium nucleatum* used this mode of transport more efficiently than others (Fig. 6A-E). It is possible that differences in adhesive forces result in preferential transport. *F. nucleatum*, which is transported the longest distance, has several cell-surface adhesins that might enhance its binding to *C. gingivalis*. Alternatively, differences in the composition of LPS or cell-surface proteins of the non-motile bacteria could have an impact on their ability to be transported as cargo. Based on our results, we propose a model where a microbial community containing gliding bacteria can use surface motility and cargo transport to find a specific niche. Once a niche is established, the bacteria can arrange in well-defined spatial structures (Fig. 7). Evidently, cargo transport plays a role in forming the spatial features of polymicrobial biofilms that contain *Capnocytophaga sp*. In the human body, such biofilms are widespread in the human gingival regions[21] and the tongue. It is known that cooperation in the form of mutualism amongst bacterial species occurs via the sharing of public goods[31]. We demonstrate that public transport enables bacterial cooperation and shapes communities of bacteria found in the human body.

Methods.

Strains and growth. Cells of *Capnocytophaga gingivalis* ATCC 33624 were used for gliding motility assays. The strain was originally isolated from the periodontal lesion of a human subject[25]. *C. gingivalis* cells were motile when grown on a medium containing

10

trypticase soy broth (TSB) 30 g/L, yeast extract 3 g/L, and 1.5% agar in a CO_2-rich anaerobic environment with high relative humidity. This was achieved by placing the bacterial cultures in an AnaeroPack System jar (Mitsubishi Gas Chemical Co.) containing 3 candles and an ignited sheet of Kimtech paper. The cells were incubated at 37˚C for 48 hours. *Fusobacterium nucleatum*, *Actinomyces sp. oral taxon-169*, *Parvimonas micra*, *Streptococcus sanguinis*, and *Veilonella parvula* were grown on a medium containing tryptic soy agar 20 g/L, brain heart infusion agar 26 g/L, yeast extract 10 g/L, hemin 5 mg/L, 5% sheep blood, and agar 4 g/L at 37˚C in an anaerobic chamber. *Prevotella oris* was grown on a medium containing the above ingredients and 1,4 dihydroxy-2-naptholic acid. *Porphyromonas endodontalis* was grown on a medium containing TSB 37 g/L, hemin 5 mg/L, $NaHCO_3$ 1 g/L, yeast extract 1 g/L, 5% sheep blood, and agar 15 g/L at 37˚C in an anaerobic chamber.

Single cell motility assay. *C. gingivalis* cells suspended in TSY broth were injected in a tunnel slide and were incubated for 5 minutes. Then, 0.25% methyl-cellulose (Methocel 90 HG Sigma-Aldrich catalog number 64680; viscosity of a 2% solution in water at 20˚C about 4000 cP) was added to the tunnel slide. After another 5 minute incubation, the gliding cells were imaged using a Nikon Plan 40x BM NA 0.65 objective (Nikon, Melville, NY) and a ThorLabs DCC1545M-GL camera (ThorLabs, Newton, NJ). Images were analyzed using a custom MATLAB (The MathWorks, Natick, MA) code. To image and analyze tethered and rotating cells, a suspension of *C. gingivalis* cells was injected into a tunnel slide and washed with TSY broth. Some of the cells tethered to glass and displayed rotation. Images of such cells were captured and analyzed using the method described above.

11

Generation of microbubbles and tracking of fluid flow patterns. About 70 µL water-insoluble surfactant Span 83 (Sorbitan sesquioleate, S3386; Sigma-Aldrich)[27] was mixed with 100 mL sterile and deionized water in a glass bottle with two inlets. Air was injected into the mixture for 1 hour after which the solution turned milky white in color. To prepare an agar pad, about 700 µl of liquid TSY agar was applied to a glass slide (#48300-026, VMR, 25X75 mm, 1.0 mm thick). A 1 µL sample of Span 83 suspension was placed on top of the agar pad and placed in a high relative-humidity chamber for about 40 minutes. 1 µL of *C. gingivalis* cells were added at the edge of the surfactant containing area. After incubation for about 20 minutes, most of the water of the 1 µL drop of cell suspension dried out. As the water dried out, the Span 83 droplet exploded and later contracted into micron sized air bubbles with surfactant walls[27]. As a swarm of gliding *C. gingivalis* approached, the buoyant bubbles moved along with it. Microbubbles formed by the surfactant were used as tracers to image the patterns of motion of the top layer of a swarm. Microbubbles were imaged using the Nikon microscope and ThorLabs camera system described above and their motion was tracked using ImageJ and a custom MATLAB script.

Cargo transport and polymicrobial interactions. In order to study cargo transport by single cells, an equal amount of *C. gingivalis* was mixed with individual non-motile bacterial species from the human oral microbiome. The mixture of cell pairs was incubated for 10 minutes after which they were injected in a tunnel slide, incubated for 5 minutes, washed with 0.25 % methyl-cellulose (defined above) and imaged using the Nikon microscope and ThorLabs camera system described above. Motion of cargo cells on the transporter cells was tracked using ImageJ and the motion of the transporter cell

12

was tracked using a custom MATLAB script. To obtain the trajectory of a moving cargo cell on a stationary transporter cell, the motion of the transporter cell was subtracted from the motion of the cargo cell using a custom MATLAB script. To test if the adhesin SprB is present on the surface of a *C. gingivalis* cell, 5 µL of affinity purified antibody raised against the *F. johnsonaie* SprB was added to 100 µL of *C. gingivalis* cells suspended in Phosphate buffered saline (PBS). After incubation for 10 minutes at 25˚C, the preparation and control with 5 µL PBS were injected into tunnel slides and were imaged using the Nikon microscope and ThorLabs camera system described above.

To image collective motion in a polymicrobial community, the cell-surface of live bacterial cells was stained with an Alexa Fluor NHS Ester (Succinimidyl Ester) dye[29]. The following bacteria-dye combinations were used: *Porphyromonas endodontalis*: Alexa 514, *Prevotella oris*: Alexa 555, *Parvimonas micra*: Alexa 568, *Actinomyces sp. oral taxon-169*: Alexa 594, *Fusobacterium nucleatum*: Alexa 633, *Streptococcus sanguinis*: Alexa 647, *Veilonella parvula*: Alexa 660. Labeling was performed by mixing 1 µL of the dye with 10 µL of the respective bacterial cell suspension, incubated in the dark for 1 hour and washed twice to remove cell-free dye. The 7 fluorescently-labeled bacteria were mixed with an equal concentration of *C. gingivalis*. 1 µL of this 8 species polymicrobial mixture was added to an agar pad and incubated for 20 minutes at high relative humidity. After the incubation, swarming was observed. To maintain an anaerobic environment, the agar pad was sealed with a cover glass and paraffin wax. Cells were imaged with a Zeiss LSM 880 Airyscan Confocal microscope in a chamber set at 37˚C. Bacteria labeled with the dyes described above were used for calibration, and spectral imaging was used to separate the 7 fluorescent signals. The images were analyzed using ImageJ and

superimposition of the fluorescent signal onto a Differential Interference Contrast (DIC) image provided the location of *C. gingivalis*. The motion of individual bacteria was tracked using ImageJ and was analyzed using a custom MATLAB script.

Imaging of fluorescent cells in a swarm. 1 µL of *C. gingivalis* cells were added to an agar pad and incubated for 20 minutes in a chamber at high relative-humidity. The edge of a swarm had smaller motile groups of cells (slugs) which were imaged using the Nikon microscope and ThorLabs camera system described above. Motion of the slugs was tracked using a custom MATLAB script. The cell-surface of live *C. gingivalis* cells was labeled with an Alexa Flour NHS Ester (Succinimidyl Ester) dye (ThermoFisher) using a method described above. The labeled cells were mixed with unlabeled cells such that the final amount of labeled cells in the mixture was 1%. The mixture was placed on an agar pad and fluorescently-labeled cells were imaged using a Zeiss LSM 880 Airyscan Confocal microscope. Motion of the cells was tracked using a custom MATLAB script.

Author Contributions: A.S., H.C.B and F.E.D. designed the experiments. A.S., V.K.P, Y.T., and S.C.Y. performed the experiments, and A.S. and H.C.B. wrote the paper.

Figure 1. Cargo-transporter relationship between bacteria of the human microbiome enables cooperation. (A) Seven non-motile bacteria stuck to the surface adhesin of a gliding bacterium *C. gingivalis* and moved along the length of that cell. Scale bar represents 1 μm. The eight bacteria shown in the matrix are some of the abundant microbial species found in a human subgingival biofilm. **(B)** The trajectory of a non-motile bacterium *Prevotella oris* transported along the length of a *C. gingivalis* cell. *P. oris* moved from one pole to another and looped back after it reached a pole. The *C. gingivalis* cell is outlined by a dotted line; color map indicates time.

Figure 2: The type IX secretion system (T9SS) and its associated rotary motor are functional in gliding bacteria of the human microbiome: (A) The center of mass of a *C. gingivalis* cell tethered to glass followed a circular trajectory. **(B)** The frequency distribution of rotation speed of a population of tethered *C. gingivalis* cells peaked around 1.5 Hz. **(C)** The frequency distribution of gliding speeds of a population of *C. gingivalis* cells peaked around 1 μm/s. **(D)** A matrix showing the similarity between T9SS and gliding motility genes of abundant bacteria of the human oral microbiome. A blue square indicates presence while a grey square indicates the absence of a gene. An e value of e^{-5} was used as the cutoff. The core gliding and core T9SS genes are shown in green and red, respectively. Bacteria shown in magenta have all green and red genes and can glide.

Figure 3. Synchronized swarm behavior of bacteria from the human microbiome. (A) A graphical representation of the use of gas bubbles to trace fluid flow patterns of a

swarm. **(B)** Time-lapse images of a swarm with gas bubbles (white) moving on top. The time lapse is in minutes. Scale bar represents 10 µm. **(C)** Trajectories of the gas bubbles moving in a circular pattern on a swarm. Color map depicts time. **(D)** A frequency distribution of the speed of gas bubbles.

Figure 4. Hierarchy within a swarm. (A) A bimodal frequency distribution of the speed of fluorescently-labeled cells moving within a swarm. The inset shows a picture of a swarm with a fluorescently-labeled cell (red) and the trajectory of that cell (green). Scale bar represents 5 µm. **(B)** The frequency distribution of speed of slugs (a small group of mobile cells). **(C)** A picture showing a slug (white) with the trajectory of its motion in green. Scale bar represents 5 µm. **(D)** An explanation for how a group of cells moves counter-clockwise. (i) A group of flexible cells (blue) moving as right handed screws. Red arrows show the direction of rotation of the cell body and green arrows show the direction of motion of a group. (ii) The leading end of one cell sticks to an external surface via multiple adhesins (orange) while the rest of the cell body keeps twisting. This produces a torsion that bends the cell towards the left of the direction of motion of the group. (iii) Cells in a group orient themselves along the cell body of the bent cell and the group moves counter-clockwise.

Figure 5. Long-range cargo transport shapes a microbial community. (A) A microbial community containing fluorescently-labeled bacteria. Eight bacteria (seven non-motile

and one motile) of the human microbiome attained a shape in which the non-motile bacteria were organized in islands by the swarming bacteria. This is a still image from the movie S13. **(B)** 20-minute trajectories of the displacement of non-motile bacteria showing that the swarming microbe transports non-motile bacteria over long distances. **(C)** Time-lapse images taken at an interval of 1 minute of a small region from Movie S13 showing that dynamically froming polymicrobial aggregates of non-motile bacteria move long distances in a swarm. Scale bar represents 5 μm.

Figure 6. (A-G) Frequency distributions of the distances that 7 non-motile bacteria were transported by a swarm of *C. gingivalis* over a time interval of 20 minutes. Bacterial species are indicated by a color code.

Figure 7. A model depicting how a gliding bacterium from the human microbiome can carry polymicrobial cargo, form mobile aggregates, and find a spatial niche where a polymicrobial biofilm can develop.

Figure S1: *F. johnsoniae* SprB antibody causes aggregation of *C. gingivalis* cells. **(A)** *C. gingivalis* cells with no antibody **(B)** *C. gingivalis* cells with anti-SprB antibody.

Figure S2: Images showing one stuck and bent cell (marked by a yellow circle) within a small group (slug) of *C. gingivalis*. Scale bar represents 5 μm.

Supplementary Movies:

Movie S1. *P. oris* transported as cargo along the length of a single *C. gingivalis* cell.

Movie S2. *F. nucleatum* transported as cargo along the length of a single *C. gingivalis* cell.

Movie S3. *P. micra* transported as cargo along the length of a single *C. gingivalis* cell.

Movie S4. *S. sanguinis* transported as cargo along the length of a single *C. gingivalis* cell.

Movie S5. *Actinomyces sp. 169* transported as cargo along the length of a single *C. gingivalis* cell.

Movie S6. *V. parvula* transported as cargo along the length of a single *C. gingivalis* cell.

Movie S7. *P. endodontalis* transported as cargo along the length of a single *C. gingivalis* cell.

Movie S8. *C. gingivalis* cell tethered to a glass surface and rotating about a fixed axis.

Movie S9. Gliding of single *C. gingivalis* cells over a glass surface.

Movie S10. A swarm of *C. gingivalis* moving in a circular fashion with layers on top of one another. Gas bubbles (bright white spheres) move along the top layer of the swarm. A less dense region with small mobile aggregates is seen near the center of the swarm.

Movie S11. Fluorescently-labeled *C. gingivalis* cells in a swarm containing both labeled and unlabeled *C. gingivalis* cells.

Movie S12. Motion of slugs found near the edge of a swarm.

Movie S13. A polymicrobial community with seven non-motile fluorescent bacteria being moved by a *C. gingivalis* (grey) resolved via spectral imaging. See Fig. 5A for a color key.

Movie S14. Time lapse images of a small region from Movie S13 shows that a polymicrobial aggregate of non-motile bacteria moves long distances in a swarm. For better contrast, *C. gingivalis* cells are represented in black while non-motile bacteria are represented by the colorkey shown in Fig. 5.

References:

1   Berg, H. C. The rotary motor of bacterial flagella. *Annu Rev Biochem* **72**, 19-54, doi:10.1146/annurev.biochem.72.121801.161737 (2003).
2   Son, K., Brumley, D. R. & Stocker, R. Live from under the lens: exploring microbial motility with dynamic imaging and microfluidics. *Nat Rev Microbiol* **13**, 761-775, doi:10.1038/nrmicro3567 (2015).
3   Tamar, E., Koler, M. & Vaknin, A. The role of motility and chemotaxis in the bacterial colonization of protected surfaces. *Sci Rep* **6**, 19616, doi:10.1038/srep19616 (2016).
4   Ottemann, K. M. & Miller, J. F. Roles for motility in bacterial-host interactions. *Mol Microbiol* **24**, 1109-1117 (1997).
5   Samad, T. *et al.* Swimming bacteria promote dispersal of non-motile staphylococcal species. *ISME J* **11**, 1933-1937, doi:10.1038/ismej.2017.23 (2017).
6   Grossart, H. P., Dziallas, C., Leunert, F. & Tang, K. W. Bacteria dispersal by hitchhiking on zooplankton. *Proc Natl Acad Sci U S A* **107**, 11959-11964, doi:10.1073/pnas.1000668107 (2010).
7   Loannou, C. C., Guttal, V. & Couzin, I. D. Predatory fish select for coordinated collective motion in virtual prey. *Science* **337**, 1212-1215, doi:10.1126/science.1218919 (2012).
8   Tamás Vicsek, A. Z. Collective motion. *Physics Reports*, 71-140 (2012).
9   Berg, H. C. Swarming motility: it better be wet. *Curr Biol* **15**, R599-600, doi:10.1016/j.cub.2005.07.042 (2005).
10   Kearns, D. B. A field guide to bacterial swarming motility. *Nat Rev Microbiol* **8**, 634-644, doi:10.1038/nrmicro2405 (2010).
11   Shrivastava, A., Roland, T. & Berg, H. C. The screw-like movement of a gliding bacterium Is powered by spiral motion of cell-surface adhesins. *Biophys J* **111**, 1008-1013, doi:10.1016/j.bpj.2016.07.043 (2016).
12   Faure, L. M. *et al.* The mechanism of force transmission at bacterial focal adhesion complexes. *Nature* **539**, 530-535, doi:10.1038/nature20121 (2016).
13   Nan, B. Bacterial gliding motility: Rolling Out a Consensus Model. *Curr Biol* **27**, R154-R156, doi:10.1016/j.cub.2016.12.035 (2017).
14   Human microbiome project, C. Structure, function and diversity of the healthy human microbiome. *Nature* **486**, 207-214, doi:10.1038/nature11234 (2012).

15   Johnson, E. L., Heaver, S. L., Walters, W. A. & Ley, R. E. Microbiome and metabolic disease: revisiting the bacterial phylum Bacteroidetes. *J Mol Med (Berl)* **95**, 1-8, doi:10.1007/s00109-016-1492-2 (2017).

16   Ley, R. E. *et al.* Obesity alters gut microbial ecology. *Proc Natl Acad Sci U S A* **102**, 11070-11075, doi:10.1073/pnas.0504978102 (2005).

17   Ley, R. E., Turnbaugh, P. J., Klein, S. & Gordon, J. I. Microbial ecology: human gut microbes associated with obesity. *Nature* **444**, 1022-1023, doi:10.1038/4441022a (2006).

18   Dubin, K. *et al.* Intestinal microbiome analyses identify melanoma patients at risk for checkpoint-blockade-induced colitis. *Nat Commun* **7**, 10391, doi:10.1038/ncomms10391 (2016).

19   McBride, M. J. & Zhu, Y. Gliding motility and Por secretion system genes are widespread among members of the phylum bacteroidetes. *J Bacteriol* **195**, 270-278, doi:10.1128/JB.01962-12 (2013).

20   Dewhirst, F. E. *et al.* The human oral microbiome. *J Bacteriol* **192**, 5002-5017, doi:10.1128/JB.00542-10 (2010).

21   Eren, A. M., Borisy, G. G., Huse, S. M. & Mark Welch, J. L. Oligotyping analysis of the human oral microbiome. *Proc Natl Acad Sci U S A* **111**, E2875-2884, doi:10.1073/pnas.1409644111 (2014).

22   Mark Welch, J. L., Rossetti, B. J., Rieken, C. W., Dewhirst, F. E. & Borisy, G. G. Biogeography of a human oral microbiome at the micron scale. *Proc Natl Acad Sci U S A* **113**, E791-800, doi:10.1073/pnas.1522149113 (2016).

23   Zhao, H. *et al.* Variations in oral microbiota associated with oral cancer. *Sci Rep* **7**, 11773, doi:10.1038/s41598-017-11779-9 (2017).

24   Teles, F. R. *et al.* Early microbial succession in redeveloping dental biofilms in periodontal health and disease. *J Periodontal Res* **47**, 95-104, doi:10.1111/j.1600-0765.2011.01409.x (2012).

25   Leadbetter, E. R., Holt, S. C. & Socransky, S. S. Capnocytophaga: new genus of gram-negative gliding bacteria. I. General characteristics, taxonomic considerations and significance. *Arch Microbiol* **122**, 9-16 (1979).

26   Kita, D. *et al.* Involvement of the Type IX secretion system in Capnocytophaga ochracea gliding motility and biofilm formation. *Appl Environ Microbiol* **82**, 1756-1766, doi:10.1128/AEM.03452-15 (2016).

27   Wu, Y., Hosu, B. G. & Berg, H. C. Microbubbles reveal chiral fluid flows in bacterial swarms. *Proc Natl Acad Sci U S A* **108**, 4147-4151, doi:10.1073/pnas.1016693108 (2011).

28   Turner, L., Ryu, W. S. & Berg, H. C. Real-time imaging of fluorescent flagellar filaments. *J Bacteriol* **182**, 2793-2801 (2000).

29   Shrivastava, A., Lele, P. P. & Berg, H. C. A rotary motor drives Flavobacterium gliding. *Curr Biol* **25**, 338-341, doi:10.1016/j.cub.2014.11.045 (2015).

30   Abby, S. S. *et al.* Identification of protein secretion systems in bacterial genomes. *Sci Rep* **6**, 23080, doi:10.1038/srep23080 (2016).

31   Drescher, K., Nadell, C. D., Stone, H. A., Wingreen, N. S. & Bassler, B. L. Solutions to the public goods dilemma in bacterial biofilms. *Curr Biol* **24**, 50-55, doi:10.1016/j.cub.2013.10.030 (2014).
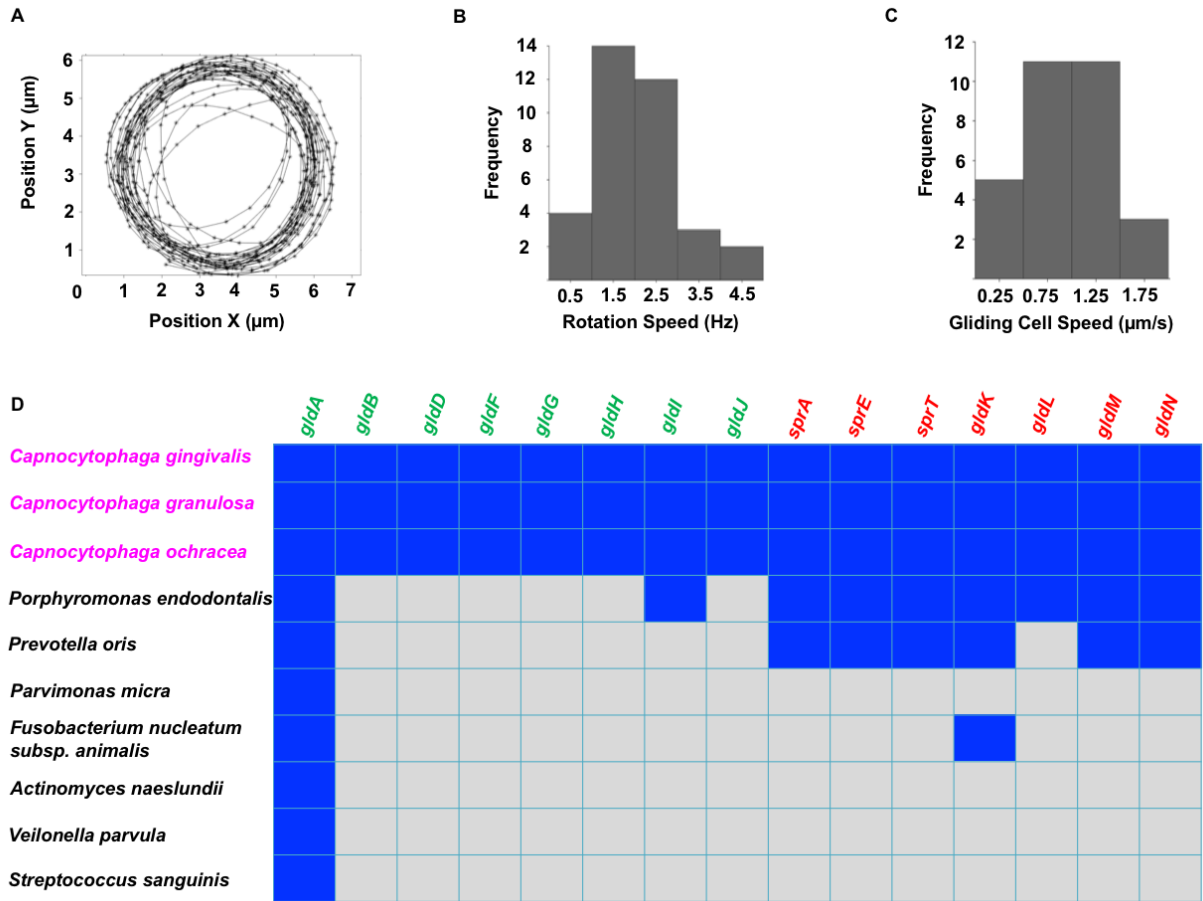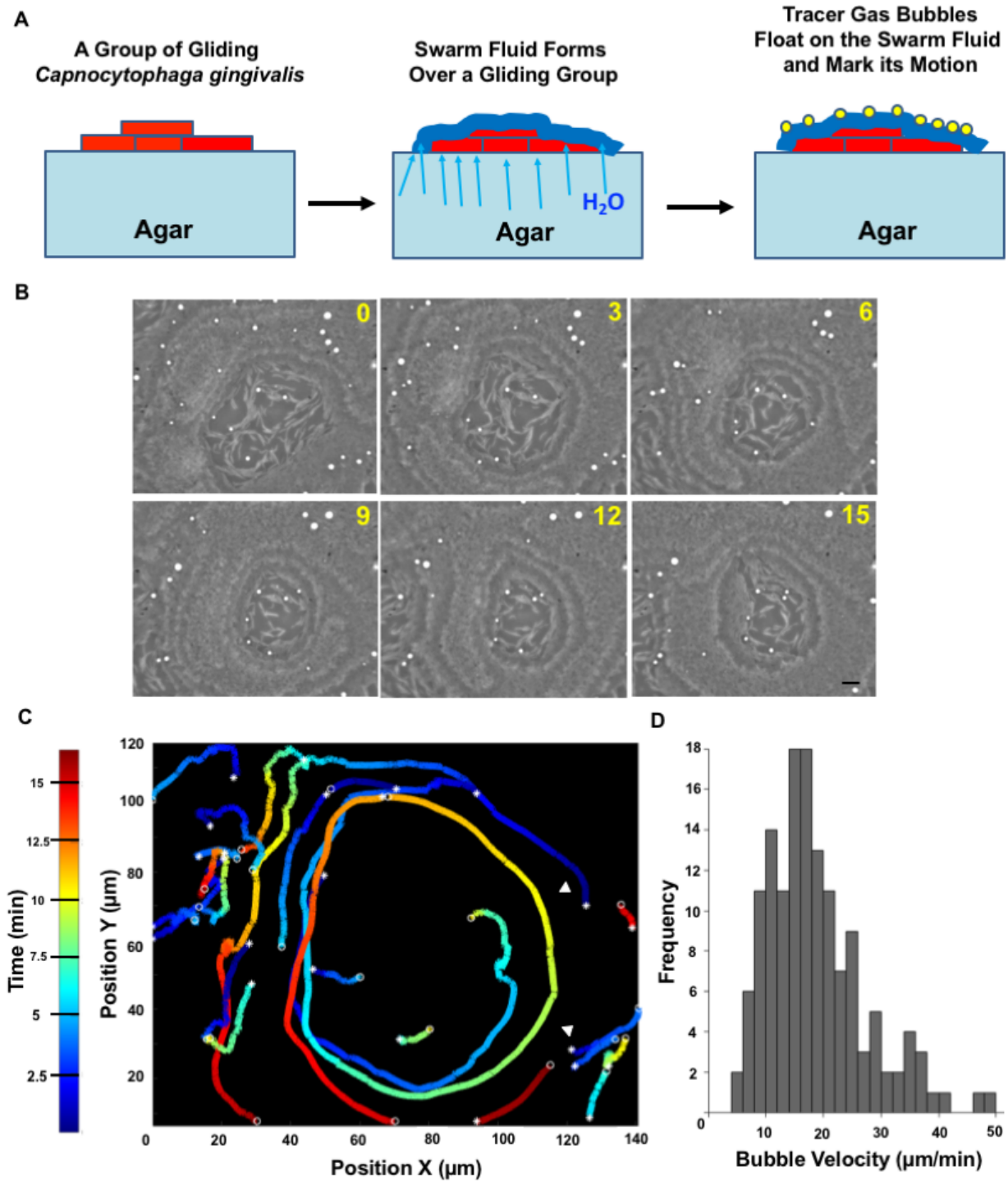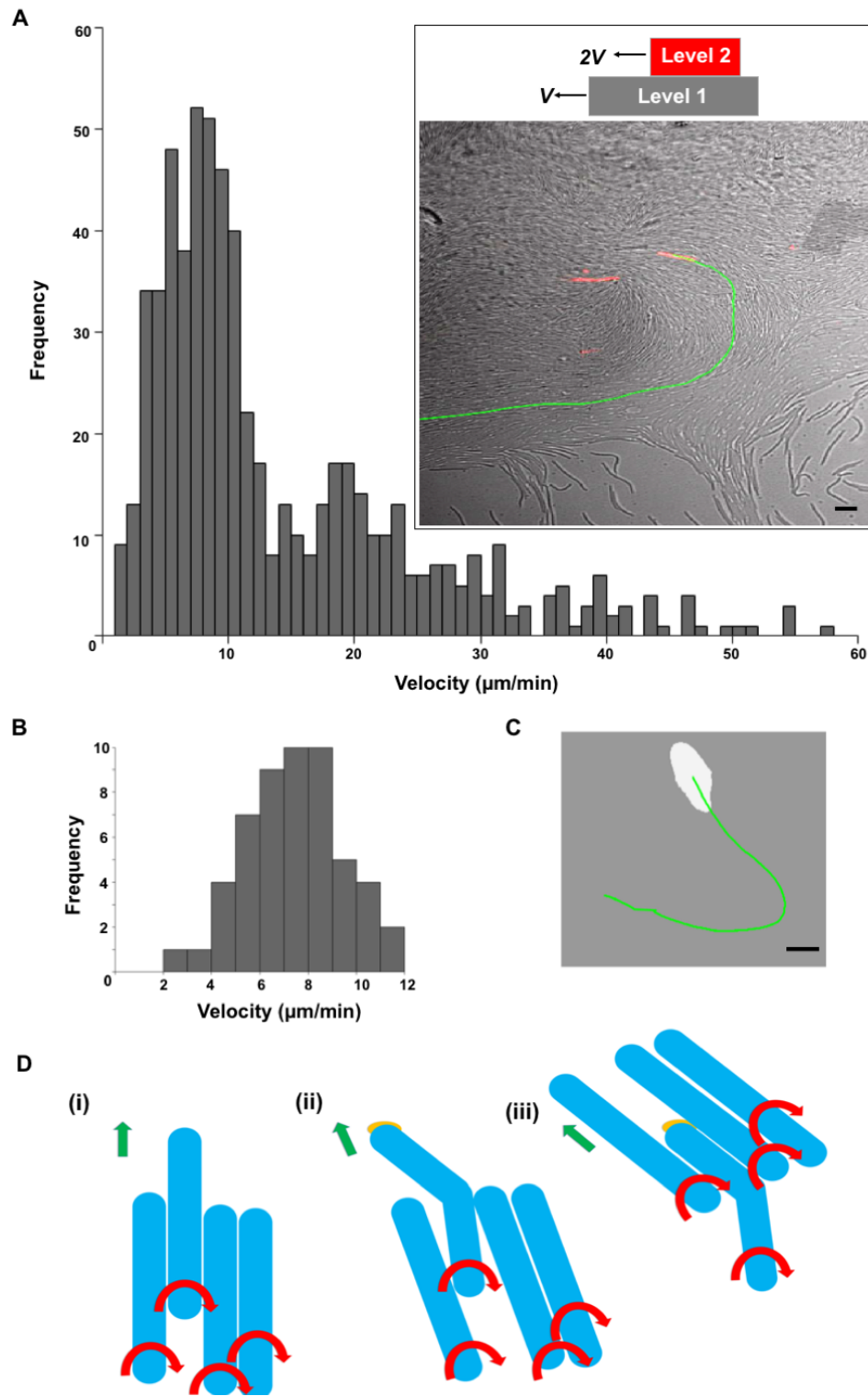
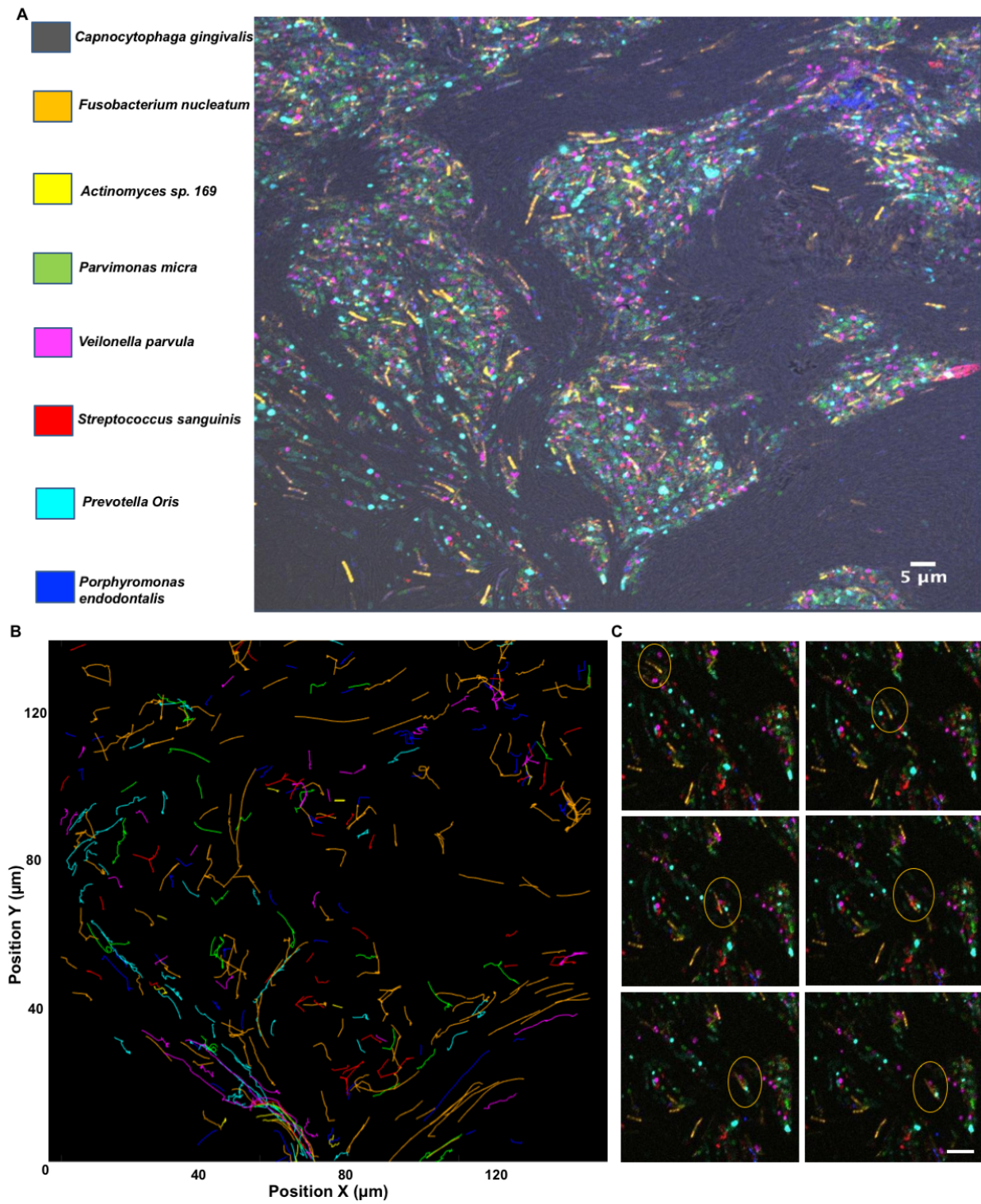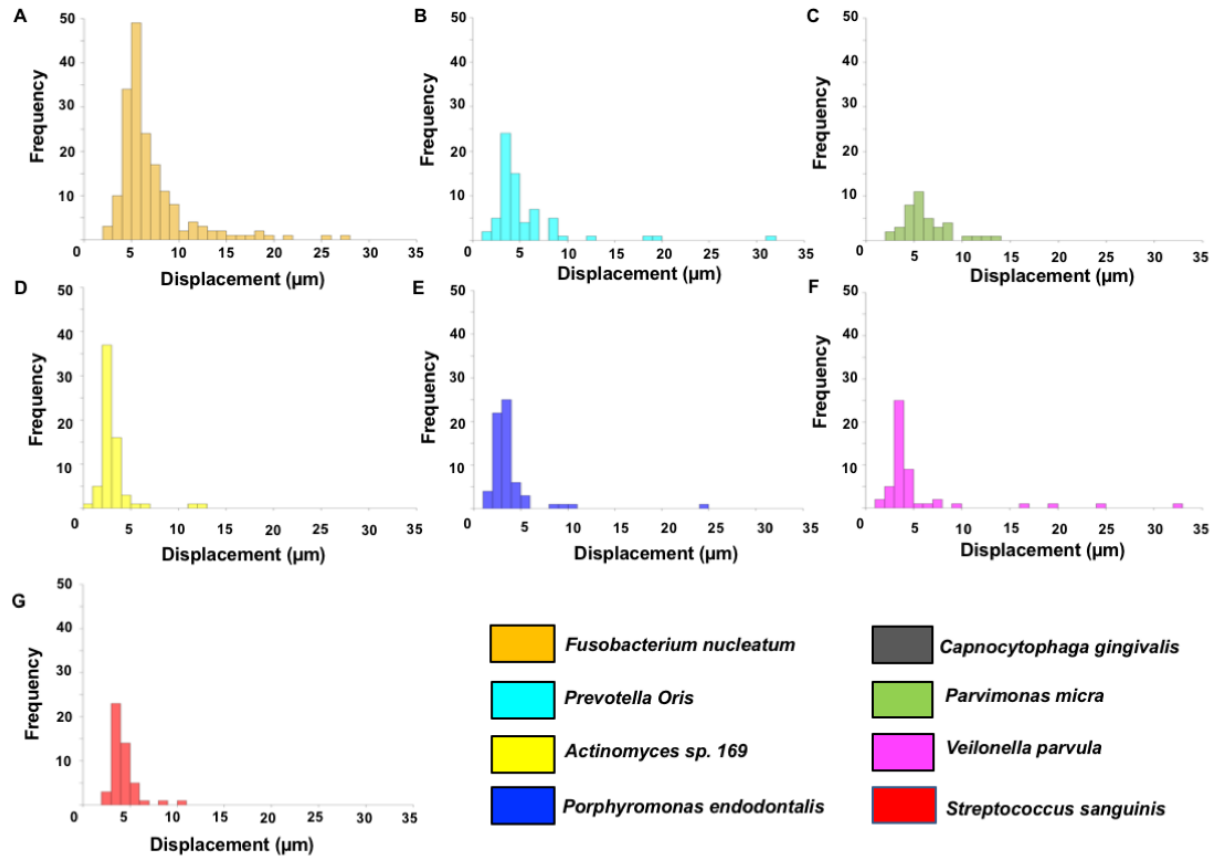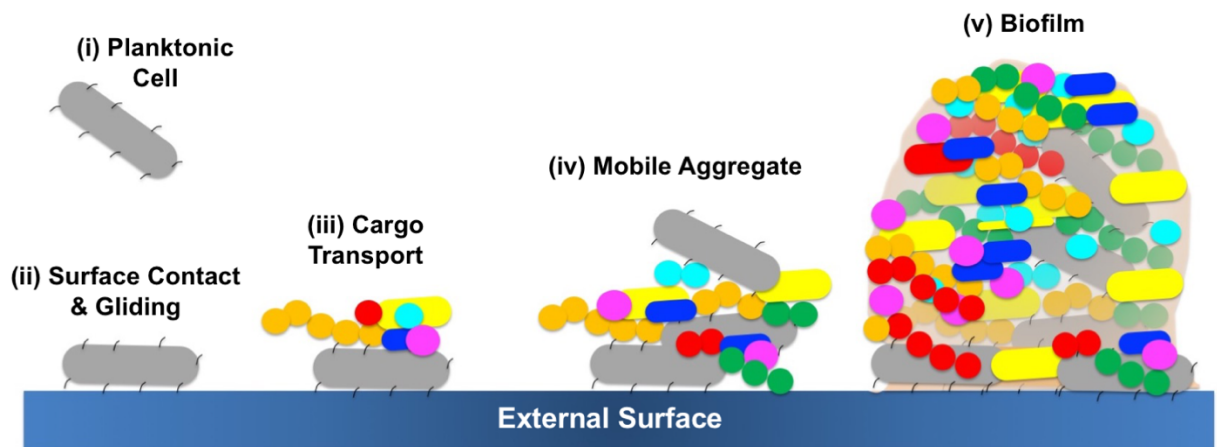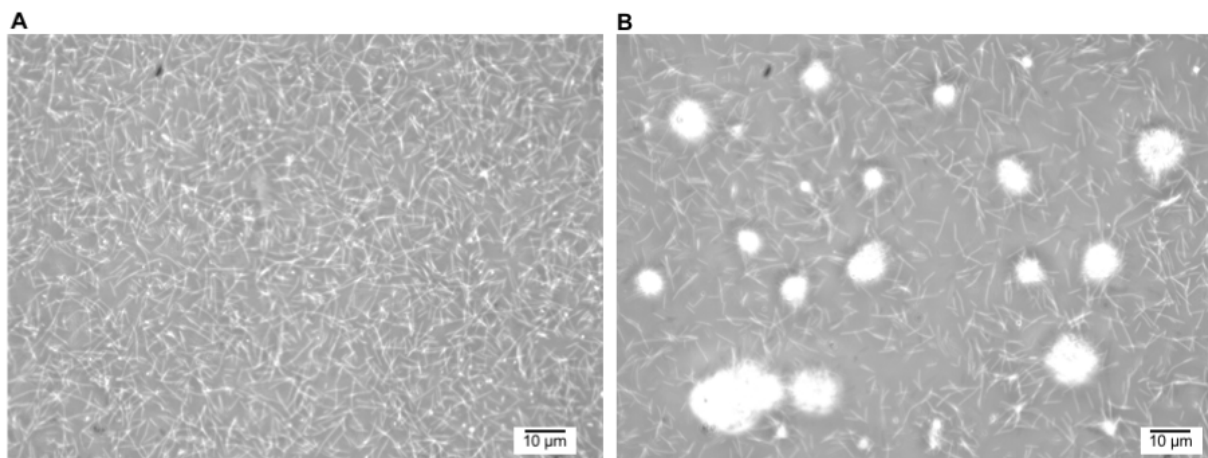**Figure 1.**
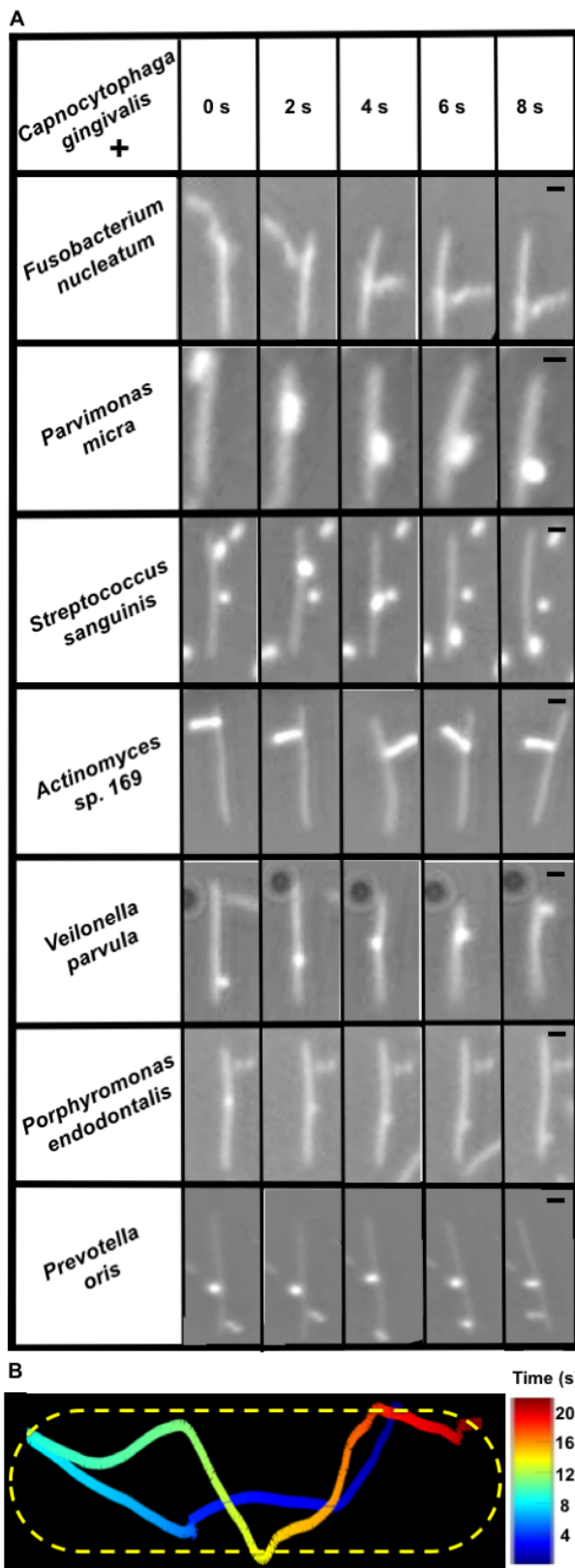
Figure 2.

Figure 3.

23

Figure 4.

Figure 5.

Figure 6.

Figure 7.

Figure S1.

Figure S2.